Journal of Applied Polymer Science

Construction of Lysozyme Exfoliated Rectorite-Based Electrospun Nanofibrous Membranes for Bacterial Inhibition

Yingfei Zhan,[1,2] Wen Zeng,[1] Guoxia Jiang,[1] Qun Wang,[3,4] Xiaowen Shi,[1] Zhehao Zhou,[1] Hongbing Deng,[1] Yumin Du[1]

[1]Department of Environmental Science, School of Resource and Environmental Science, Wuhan University, Wuhan 430079, China
[2]Hubei-MOST KLOS & KLOBME, Wuhan University Stomatological Hospital, Wuhan University, Wuhan 430079, China
[3]Department of Chemical and Biological Engineering, Iowa State University, Ames, Iowa 50014
[4]Department of Civil, Construction and Environmental Engineering, Iowa State University, Ames, Iowa 50014
Correspondence to: H. Deng (E-mail: hbdeng@whu.edu.cn or alphabeita@yahoo.com)

ABSTRACT: Lysozyme (LY) exfoliated rectorite (REC) based electrospun nanofibrous membranes with enhanced bacterial inhibition ability and thermostability were fabricated via electrospinning. All the obtained membranes exhibited better fiber shape and three-dimensional structure, which could be observed by scanning electron microscopy. Energy-dispersive X-ray analysis, X-ray photoelectron spectroscopy, and Fourier transform infrared (FTIR) spectrum denoted the existence of LY and REC in the composite membranes. Besides, the FTIR results suggested that there were interactions between REC and polyvinyl alcohol (PVA)/LY chains. Small angle X-ray diffraction indicated that REC was exfoliated by PVA and LY chains. In addition, the exfoliation of REC was directly confirmed by transmission electron microscopy. According to Brunauer-Emmett-Teller surface area test results, PVA/LY/REC membranes had higher surface area than that of PVA/LY membranes. The performance tests showed that both the thermal stability and antibacterial activity of the composite membranes were enhanced after adding REC. © 2014 Wiley Periodicals, Inc. J. Appl. Polym. Sci. **2015**, *132*, 41496.

KEYWORDS: composites; electrospinning; fibers; membranes

Received 25 April 2014; accepted 29 August 2014
DOI: 10.1002/app.41496

INTRODUCTION

In 2011, European Food Safety Authority (EFSA) pointed out that bentonite (dioctahedral montmorillonite, a kind of layered silicate) had no obvious toxicity when it used as a feed additive for the reduction of milk aflatoxin.[1] Besides, it was also environment friendly because it was a natural soil component ubiquitous in the environment.[1] Rectorite (REC), with the structure and chemical components similar to other layered silicates, has been reported with larger interlayer distance, easier intercalation and exfoliation process,[2] better separable layer thickness and layer aspect ratio than montmorillonite.[3] It can be selected as an ideal candidate for biomedical applications and food packaging in future.

Till now, REC has a variety of applications comprising catalysis,[4,5] gene delivery, drug controlled release, adsorption[5,6] and bacteria inhibition.[3] Interestingly, REC itself had no antibacterial ability,[7] but when it was blended with antibacterial cationic polymers, such as chitosan (CS), the obtained composites showed enhanced antimicrobial activity.[8] The main reason was that the polymer chains could be intercalated into the interlayer of REC,[6,9,10] and the polymer/REC composites exhibited obvious capability of adsorbing bacteria and inhibiting their growth.[3,7,11,12] This phenomenon was called the synergetic bacteria inhibition.[7,11,12] On the basis of this consideration, lysozyme (LY), as a kind of antibacterial protein, was selected to cooperate with REC to fabricate protein-layered silicate composites. And the composites were tested to investigate whether they had better antimicrobial activity or not.

As we know, LY is an important component of the innate immune system of the hosts.[13] It owns significant antibacterial activity against a broad spectrum of bacterial, fungal, and viral pathogens.[14] Additionally, LY shows a wide range of bacteriostatic activity, including both Gram-positive bacteria and part of Gram-negative bacteria,[15] because it can make bacteria sensitive to osmotic lysis by degrading peptidoglycan.[16] Moreover, the excellent characteristics of LY, including the high stability, wide suitable pH range, and significant resistance to heat and cold, make it outstanding among numerous natural antibacterial substances.[14] Furthermore, immobilized LY, compared with free

LY, apparently exhibits improved reusability and stability to environmental changes.

Various methods applied to immobilize LY include protein adsorption onto nanoparticles,[17–19] layer-by-layer assembly technique,[20,21] surface grafting modification[22] and the embedding methods,[23] and so on. Considering the weakness of those methods, such as the craft complicacy, the technical difficulties and the toxicity of raw materials, more efforts have been made to explore new methods of immobilizing LY.

Electrospinning, as a simple and effective technology, can produce continuous and uniform nanofibers with diameters ranging from micrometers to nanometers.[24] Thus, it can be applied to immobilizing LY and REC into nanofibrous membranes. The LY-REC based composite fibers are expected to be endowed with the characteristics of nanofibers including ultrafine diameter, high surface area-to-volume ratio, three-dimensional (3D) nanofibrous structure and excellent thermal stability,[12] and so on. Because of the poor electrospinnability of LY-REC solutions, polyvinyl alcohol (PVA) was added into the solutions to assist fiber formation.

In this study, a series of PVA/LY/REC composite nanofibrous membranes with different composition ratio were fabricated via electrospinning. The morphology, structure, thermal stability, and antibacterial activity of the nanofibrous membranes were examined.

EXPERIMENTAL

Materials

Poly(vinyl alcohol) (PVA, $M_w = 9 \times 10^4$) was provided by Sigma Aldrich Chemical Reagent Co. Calcium rectorite (Ca^{2+}-REC) refined from the clay minerals was provided by Hubei Mingliu Co. (Wuhan, China). Lysozyme (LY, activity 25,000 U mg^{-1}) was obtained from Amresco Co. Other chemicals of analytical grade were used as received without any further purification. *Escherichia coli* and *Staphylococcus aureus* were obtained from State Key Laboratory of Agricultural Microbiology of Huazhong Agricultural University (Wuhan, China), and nutrient agar and nutrient broth were supplied by Qingdao Rishui Biological Technology Co. (Qingdao, China). All aqueous solutions were prepared using purified water with a resistance of 18.2 MΩ cm.

Preparation of PVA/LY and PVA/LY/REC Blend Solutions

A 10% PVA solution was prepared by dissolving PVA powder into purified water with gentle magnetic stirring for 4 h under 60°C water bath. A 5% LY solution was prepared by adding LY powder into purified water. PVA/LY mixed solutions were obtained by mixing 10% PVA and 5% LY together to achieve PVA/LY mixture at 80/20, 70/30, and 60/40 mass ratios, respectively. Then 1 wt % REC was added into each as-prepared PVA/LY solution to get PVA/LY/REC solution. Finally, the mixtures were kept stirring for 48 h at room temperature. The concentrations of all above solutions were expressed in wt/wt %.

Fabrication of Nanofibrous Membranes

The electrospinning solution was fed into a plastic syringe pump equipped with a needle having an internal diameter of 0.8 mm. The positive electrode of a high voltage power supply (DW-P303-1ACD8, Tianjin Dongwen Co., China) was clamped to the metal needle tip of the syringe. The constant flow rates were modulated at 1 mL/h using by a syringe pump (LSP02-1B, Baoding Longer Precision Pump Co., China). The tip-to-collector distance was 15 cm with the applied voltage of 15 kV. The as-spun fibers were collected by a grounded collector covered with aluminum foil. The ambient temperature and relative humidity were kept at 25°C and 45%, respectively. The prepared samples were dried in vacuum at room temperature for 24 h to remove the trace solvent.

Characterization

Field emission scanning electron microscopies (FE-SEM) and energy-dispersive X-ray (EDX) spectroscopy images were obtained by Hitachi S-4800 (S-4800, Hitachi, Japan). Field emission transmission electron microscopies (FE-TEM) were obtained by JEM-2100 (HR, JEOL, Japan). The nanofibrous membranes (3×3 mm^2) for SEM examination were sputter coated with gold beforehand and for TEM were prepared by electrospinning the blending solutions onto copper grids directly. X-ray photoelectron spectroscopy (XPS) was recorded on an axis ultra DLD apparatus (Kratos, UK) to detect the surface elements of nanofibrous membrane samples (5×5 mm^2). The nanofibrous membranes were sheared, pestled, and tableted to prepare disks (diameter = 1 cm) for Fourier transform infrared (FTIR) detection, and FTIR spectra were identified by Nicolet170-SX (Thermo Nicolet) in the wavenumber range of 4000–400 cm^{-1}. The X-ray diffraction (XRD) was carried out using a diffractometer type D/max-rA (Rigaku Co., Japan) with Cu target and Ka radiation ($\lambda = 0.154$ nm). The nanofibrous membranes were cut into square samples (1×1 cm^2) for XRD determination. The scanning rate for the wide-angle X-ray diffraction (WAXRD) was 1°/min and the scanning scope of 2θ was 6–60°. For small-angle X-ray diffraction (SAXRD), the scanning rate was 1°/min and the scanning scope of 2θ was between 2° and 9°. The thermal stability of nanofibrous membranes (100 mg) was determined by differential scanning calorimetry (DSC204 F1, Zetzsch, Germany) which were heated up twice from 50 to 500°C with a heating rate of 10 °C/min under nitrogen flow (20 mL/min) to remove the heat history and thermo-gravimetric analysis (TGA, Pyris 1 TGA, PerkinElmer) with a temperature range of 20–500°C. The Brunauer-Emmett-Teller (BET) surface area and pore volume (BJH method) of the nanofibrous membranes were characterized by nitrogen adsorption using a surface area and pore size analyzer (Quantachrome NOVA 4200e) at 77K and a relative pressure (P/P_o) range of 0.005–0.99.

Microbial Inhibition Assay

Inhibition rate of the nanofibrous membranes against bacteria was measured as our previous literature.[3] Disk-diffusion test was conducted to investigate the inhibitory effect of the membranes. Gram-negative bacteria *Escherichia coli* (*E. coli*) and Gram-positive bacteria *Staphylococcus aureus* (*S. aureus*) were selected as the representative bacteria. A total of 50 μL of diluted bacterial suspension with the concentration of 5.0–10.0×10^5 CFU/mL was inoculated into the meat-peptone broth and then coated uniformly. The nanofibrous membranes were

cut into disks with aluminum foil (diameter = 6 mm) and sterilized under an ultraviolet radiation lamp for 30 min. After that, the disks were placed on the surface of meat-peptone broth and cultured at 37°C for 24 h. The inhibition zones diameters were measured with a tolerance of 1 mm. Each sample was repeated three times.

RESULT AND DISCUSSION

Morphology of the Nanofibrous Membranes

Figure 1 shows the FE-SEM images of nanofibrous membranes fabricated from different solutions. It is well known that the uniformity of electrospun nanofibers is markedly influenced by the polymer solution properties and the electrospinning processing parameters.[25] Thus, nanofibrous membranes fabricated from a 10% PVA solution were chosen as control [Figure 1(a)]. Obviously, due to the outstanding film-forming and spinnability of PVA, the pure PVA nanofibrous membrane mainly consisted of thin cylindrical nanofibers with uniform shape and extraordinary 3D structure.

It was reported that the addition of cationic and anionic polyelectrolytes could increase the conductivity of polymer solutions and resulted in a thinner fiber diameter.[26] Below the isoelectric point, LY is a cationic protein over a wide pH range. Therefore, the morphology and diameter of electrospun fibers were expected to be affected by the weight ratio of PVA/LY. Figure 1(b–d) show the images of nanofibrous membranes electrospun from PVA/LY solutions at different mass ratios, and a few spindle-like beads are observed among them, which may be caused when the solution viscosity has decreased with reducing PVA amount in the blend solutions. Our previous study indicated that the addition of PVA exhibited a significant effect on the rheological behavior of the composite solutions, and PVA could strongly enhance the intermolecular interactions.[27] Besides, the diameter gradually decreased with the increasing LY content in the blend solutions, whereas more beads with smaller diameter were obtained in the composites. LY is an ionic polyelectrolyte, causing a higher charge density on the surface of the ejected jet formed during electrospinning, so higher elongation forces are imposed on the jet than that without LY under the electrical field.

Moreover, the addition of REC could evidently improve the shape and 3D structure of nanofibrous membranes [Figure 1(e–f)]. Compared with the nanofibrous membranes electrospun from solutions with the same mass ratio of PVA/LY, those nanofibrous membranes containing 1 wt % REC possessed less spindle-like beads and their average diameter was much smaller. The reason was various. First, when the concentration of polymers in the electrospinning solution was lower, the obtained nanofibers displayed thinner diameters.[12] Second, adding REC could increase the density of electrospinning droplets and consequently increase the flying speed of the droplets, which was propitious to generate thinner nanofibers. Third, the conductivity and viscosity of the electrospinning solution would also affect the formation of nanofibers.[12] Bigger and more protuberances would be among the nanofibrous membranes because of the high positive charge of the composites.[20] In contrast, the negative charge of REC neutralized the positive charge of LY, which contributed to the decrease of beads.

EDX and XPS Spectra

XPS and EDX analysis were performed to investigate the surface composition of the nanofibrous membranes. As we know, the main components of REC are Si, Al, and Na elements. In the EDX spectroscopy of PVA/LY/REC composite nanofibrous membranes [Figure 2(a)], the characteristic peaks of Na, Si, and Al could be easily observed, demonstrating that REC was successfully incorporated into the composite nanofibrous membranes. Besides, the characteristic peak of S revealed that LY was also existed in the composite nanofibrous membranes.

Figure 2(b and c) present the XPS data of PVA/LY and PVA/LY/REC composite membranes, respectively. For PVA/LY membranes [Figure 2(b)], the presence of N element on the surface of the composite membranes was attributed to nature of proteins, indicating a combination of PVA and LY. In the spectrum [Figure 2(c)] of PVA/LY/REC membranes, Si element could be detected on the surface of the membranes, which further confirmed the presence of REC. In addition, Si peak showed two significant peaks for the curve fit at 103.7 eV (silicon dioxide) and 99.5 eV (Si-Si).

FTIR Spectra

Figure 3 displays the FTIR spectra of the raw materials and the composite nanofibrous membranes. PVA nanofibrous membranes showed absorption bands at 3383, 2941, 1734, 1098, and 850 cm^{-1}, which denoted the O–H, $–CH_2$, C=O, C–O, and C–C resonances, respectively.[28] Except for a few new peaks, the spectra of the PVA/LY membranes [Figure 3(a)] and PVA/LY/REC membranes [Figure 3(b)] were similar to the spectrum of PVA membranes.

The spectrum of LY contained two characteristic peaks, the amide I band (near 1657 cm^{-1}) was relevant to the C=O stretching mode, whereas the amide II band (near 1527 cm^{-1}) was due to the stretching mode of N—H vibrations.[29] REC exhibited dominant peaks at 467 and 546 cm^{-1} assigned to Si-O bending vibration, 910 and 3643 cm^{-1} bands stood for -OH vibration, 1025 and 1050 cm^{-1} represented for Si-O stretching vibration band, and 1650 cm^{-1} caused by the bending vibration of H_2O.[7]

Obviously, the spectrum of the PVA/LY/REC membranes [Figure 3(b)] had the Si—O bending vibration at 546 and 467 cm^{-1}, which verified that REC was in the composite nanofibrous membranes. This result was identical with that of the former elements analysis. Besides, in Figure 3(b), the band of REC at 3643 cm^{-1} disappeared, which implied that the —OH of REC reacted with the groups of PVA or LY: the —OH of REC might form ether bond with the —OH of LY or PVA, or possibly generated hydrogen bond with the amino group of LY.[12] Evidently, the bands of hydroxyl stretching became broader with adding LY, which indicated that hydrogen bond could be formed between the —OH of PVA and LY. Moreover, the N—H bonded to O—H vibration band at 3448 cm^{-1} in the spectra of PVA/LY or PVA/LY/REC nanofibrous membranes shifted toward lower frequency no matter what it blended with, which revealed that the $—NH_2$ and —OH groups of LY could have formed

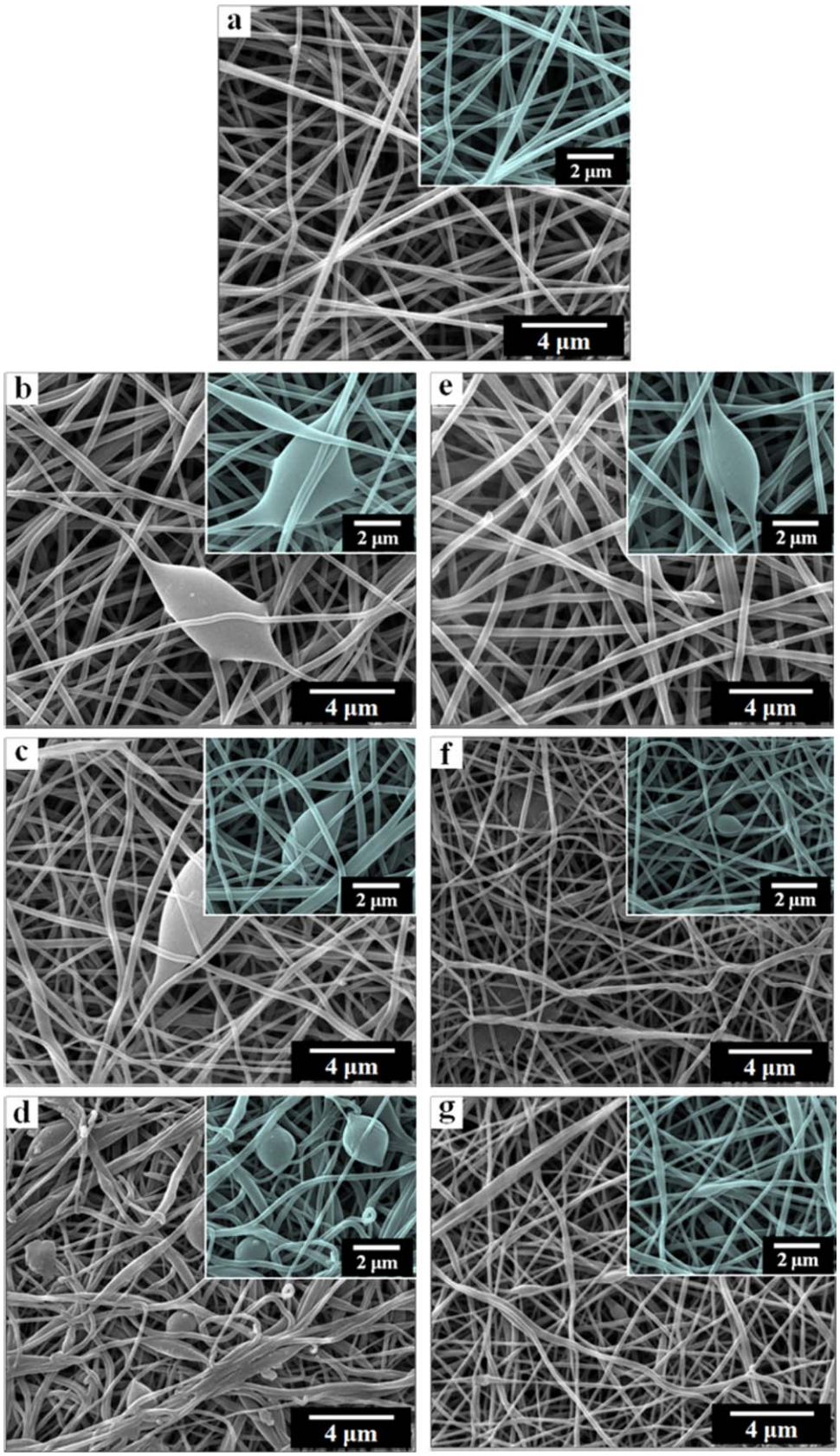

Figure 1. FE-SEM images of nanofibrous membranes electrospun from solutions with various PVA/LY mass ratios: (a) 100/0, (b) 80/20, (c) 70/30, and (d) 60/40, and nanofibrous membranes electrospun from solutions with various PVA/LY mass ratios containing 1 wt % REC: (e) 80/20, (f) 70/30, and (g) 60/40. [Color figure can be viewed in the online issue, which is available at wileyonlinelibrary.com.]

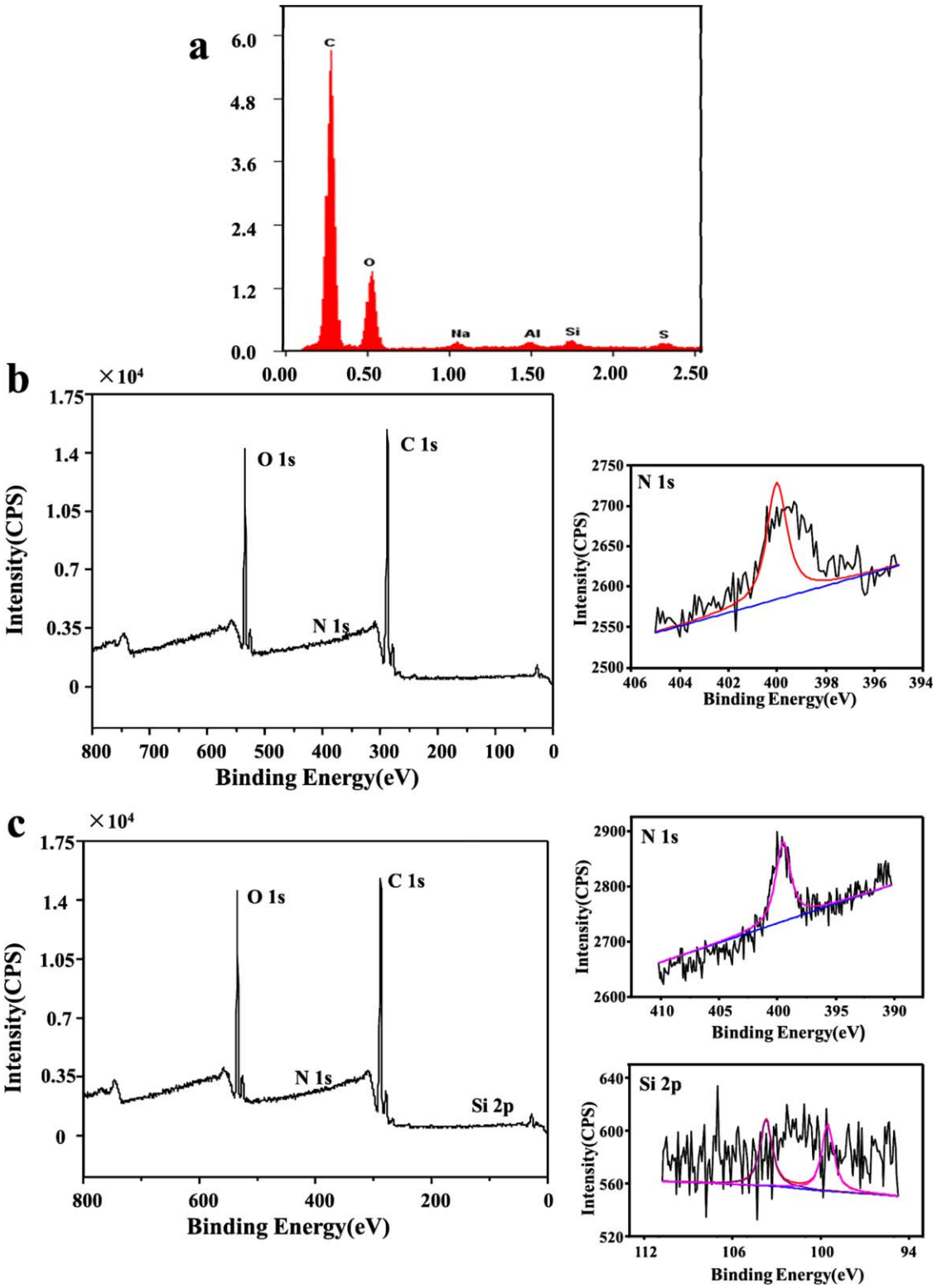

Figure 2. (a) EDX spectrum of selected composite nanofibrous membranes electrospun from solutions containing 1 wt % REC with PVA/LY weight ratio of 80/20 and XPS spectra of nanofibrous membranes fabricated from: (b) PVA/LY (80/20, the right figure was for N 1 s narrow scans) and (c) PVA/LY/REC (80/20, 1 wt % REC, the right figure was for N 1 s and Si 2p narrow scans). [Color figure can be viewed in the online issue, which is available at wileyonlinelibrary.com.]

hydrogen bonds with the —OH group of REC and PVA.[12] There might also be intermolecular and intramolecular hydrogen bond action in LY molecules.

WAXRD Analysis

Figure 4 presents the WAXRD patterns of the bulk REC and PVA powder, PVA/LY and PVA/LY/REC composite nanofibrous

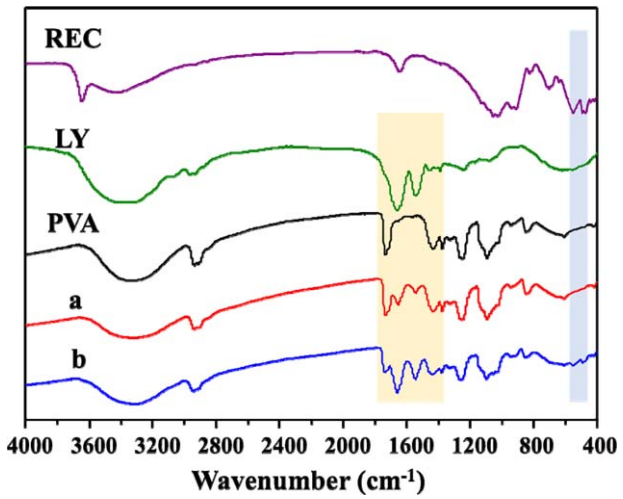

Figure 3. FTIR spectra of bulk materials and the nanofibrous membranes electrospun from solutions: (a) with PVA/LY weight ratio of 80/20, (b) containing 1 wt % REC with PVA/LY weight ratio of 70/30. [Color figure can be viewed in the online issue, which is available at wileyonlinelibrary.com.]

membranes. The diffraction of REC consisted of 7.09°, 17.73°, 20.01°, 27.44°, 28.68°, 35.35°, and 54.36°. PVA exhibited major crystal peak around 19.84°, and the typical crystal peaks of LY were 31.63° and 45.39°. Compared with the spectrum of pure PVA, the crystalline peaks at 20.10° in the spectrum of PVA/LY/REC composite membranes became wider, clearly demonstrating that the interaction among PVA, LY, and REC might induce the crystallization of PVA and LY.[7]

SAXRD Analysis and TEM Micrographs

In order to verify whether the chains of the PVA and LY polymers could intercalate into the REC interlayer or not, SAXRD patterns of the bulk materials and the composite nanofibrous membranes were investigated (Figure 4). According to the SAXRD results, the interlayer distance of REC was 2.32 nm, calculated by the Bragg's equation. Compared with the spectrum of REC, no peak could be found in the patterns of PVA/LY/REC composite nanofibrous membranes. As we know, if the intercalation of the polymer chains into the interlayer of the layered silicate occurred, the SAXRD peak of the composites would shift to a smaller angle. In addition, if the REC layers were exfoliated completely, no diffraction peaks could be observed because of the disorder of sheets or the larger space of the layers beyond the SAXRD resolution.[30] As an intercalator, PVA with long alkyl chains could effectively enlarge the distance of the interlayer of REC in that alkyl tails could move the platelets apart within a certain limit, consequently reduced the cohesive forces between layers and conduced to the insertion of other polymer chains.[31] However, at the same time, these alkyls sterically diminished the opportunity for the polymer to interact with REC surface, which hindered the further intercalation and exfoliation.[31] But the electrostatic interaction could take place when cationic LY anchored to the interlayer space of electronegative REC because of the good cation exchange capacity of REC,[2,32,33] which could lead to the swelling of the molecular chains.[34] Consequently, the distance of the interlayer became larger and larger until the layered structure was destroyed, in other words, REC was exfoliated.[34]

Figure 5(a,b) show the inner structure of PVA/LY/REC nanofibrous membranes. In general, REC, which showed black granules or crumbs in the nanofibers, could equably disperse inner the nanofibers (showed as area inside the ellipses in Figure 5). But there were still some big granules of REC remaining in the nanofibers (showed as where the arrows pointing to in Figure 5). Figure 5(c), a large layered structure substance in nanoscale, was the TEM microscopy of REC. The direct confirmation of the intercalation or exfoliation can be observed by comparing Figure 5(d) with Figure 5(c). More specifically, the two red dashed lines along the cross section of REC layers were not parallel, whereas the REC that was not exfoliated possessed parallel layers.[35,36]

Surface Area and Adsorption–Desorption Isotherms

As the table inside Figure 6 shows, the surface area of the PVA/LY/REC nanofibrous samples were slightly higher than that of PVA/LY membranes, which indicated that the addition of REC

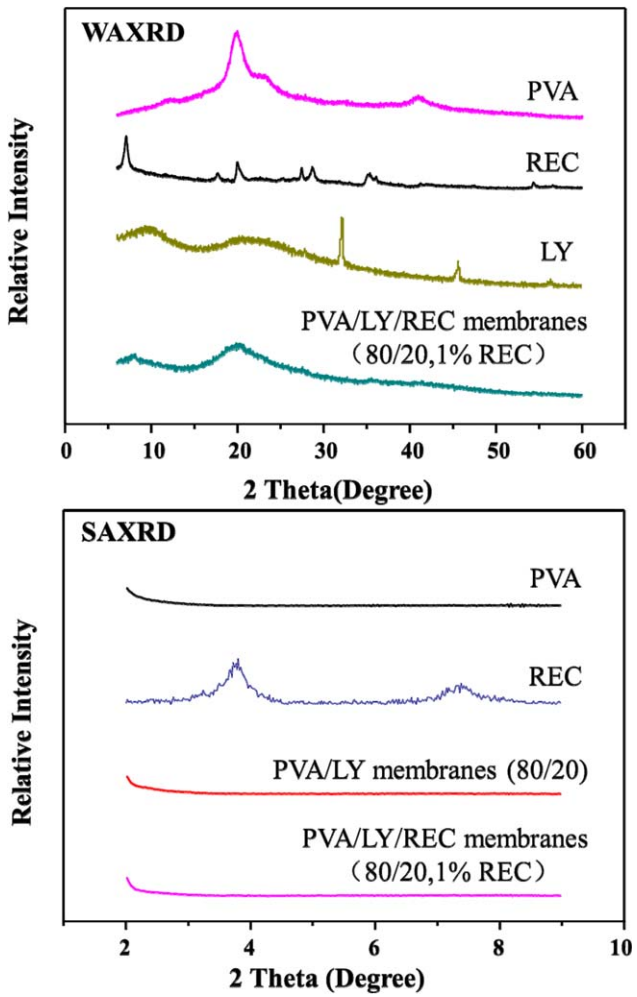

Figure 4. WAXRD and SAXRD patterns of the raw materials and composite nanofibrous membranes. [Color figure can be viewed in the online issue, which is available at wileyonlinelibrary.com.]

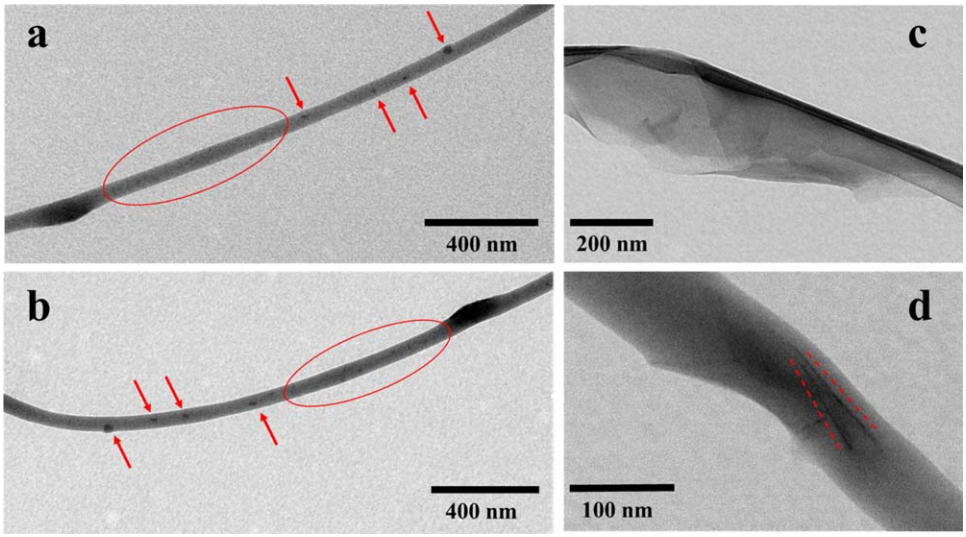

Figure 5. TEM micrographs: (a), (b), (d) the composite nanofibrous membranes electrospun from solutions containing 1 wt % REC with PVA/LY weight ratio of 80/20 and (c) REC. [Color figure can be viewed in the online issue, which is available at wileyonlinelibrary.com.]

could increase the surface area of composite nanofibrous membranes. Compared with that of PVA/REC membranes, PVA/LY/REC membranes had slightly larger surface area. This was due to the intercalation reaction and the exfoliation of REC caused by LY chains. In addition, the quantity adsorbed of the PVA/LY/REC composite nanofibrous membranes was larger than that of the other two composite nanofibrous membranes from start to finish, which might be related with the intercalation and exfoliation reaction between polymer chains and the interlayer of REC.

Thermal Properties

The thermal stability of composite nanofibrous membranes was evaluated by DSC and TGA analysis (Figure 7). Regarding to

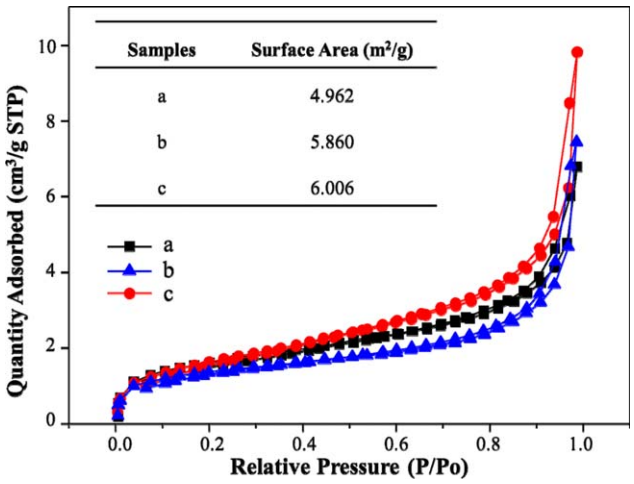

Figure 6. The nitrogen adsorption–desorption isotherms and surface area data of the composite nanofibrous membranes electrospun from solutions: (a) with PVA/LY weight ratio of 80/20, (b) containing 1 wt % REC with PVA/LY weight ratio of 100/0, and (c) containing 1 wt % REC with PVA/LY weight ratio of 80/20. [Color figure can be viewed in the online issue, which is available at wileyonlinelibrary.com.]

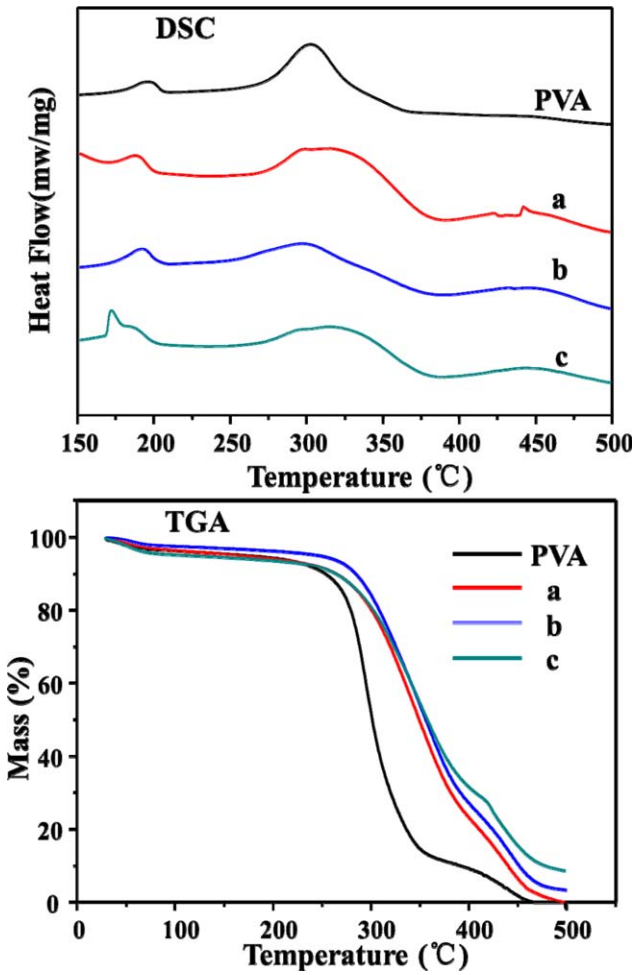

Figure 7. DSC and TGA thermograms of bulk and the composite nanofibrous membranes electrospun from solutions: (a) with PVA/LY weight ratio of 70/30, (b) containing 1 wt % REC with PVA/LY weight ratio of 80/20, and (c) containing 1 wt % REC with PVA/LY weight ratio of 70/30. [Color figure can be viewed in the online issue, which is available at wileyonlinelibrary.com.]

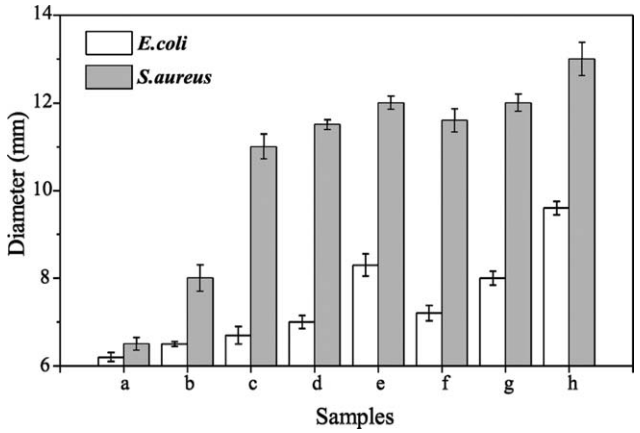

Figure 8. Antimicrobial activities against *E. coli* and *S. aureus* of: (a) aluminum foil, and nanofibrous membranes fabricated from solutions with various PVA/LY mass ratios: (b) 100/0, (c) 80/20, (d) 70/30, and (e) 60/40; and nanofibrous membranes electrospun from solutions with various PVA/LY mass ratios containing 1 wt % REC: (f) 80/20, (g) 70/30, and (h) 60/40.

DSC analysis, it could be noted that the appearance of an exothermic event at 194°C in the spectrum of bulk PVA because of the PVA crystallization. However, the results of PVA/LY/REC composite nanofibrous membranes were slightly lower than 194°C in that the addition of LY might slightly weaken the thermal stability of the membranes. In contrast, the peaks around 300°C emerged the opposite trend. The reason would be that the addition of REC could enhance the thermal stability of the composite membranes.

PVA chains would form conjugated polyene after the water was removed.[27] Consequently, three weight loss peaks could be observed in the TGA analysis for bulk PVA (Figure 7). The first peak between 20 and 300°C was attributed to water loss, the second peak between 300 and 350°C was corresponded to the decomposition of PVA, and the third peak between 350 and 500°C appeared owing to the carbonization of the degraded products to ash. For PVA/LY nanofibrous membranes, they exhibited similar curves to that of PVA/LY/REC nanofibrous membranes. The T_{max} of PVA/LY nanofibrous membranes was slightly lower than that of PVA/LY/REC nanofibrous membranes. Here, T_{max} means the temperature when the rate of weight loss reached a maximum. This phenomenon also indicated that the thermal stability was improved with the addition of REC. Generally, REC containing mica layer with the high temperature resistance might contribute to the enhancement of thermal stability.[37]

Antimicrobial Activities

The antibacterial activity is the most valuable property in the field of food and biomedical application,[38] as food engineering and biomedical materials have to sterilize or prevent from many microorganisms. The antibacterial activity assay was measured with inhibition zone method (Figure 8).

As negative controls, the aluminum foil and PVA nanofibrous disks [Figure 8 (a,b)] exhibited a little inhibition ability. The application of PVA as a polymer matrix is a popular choice in

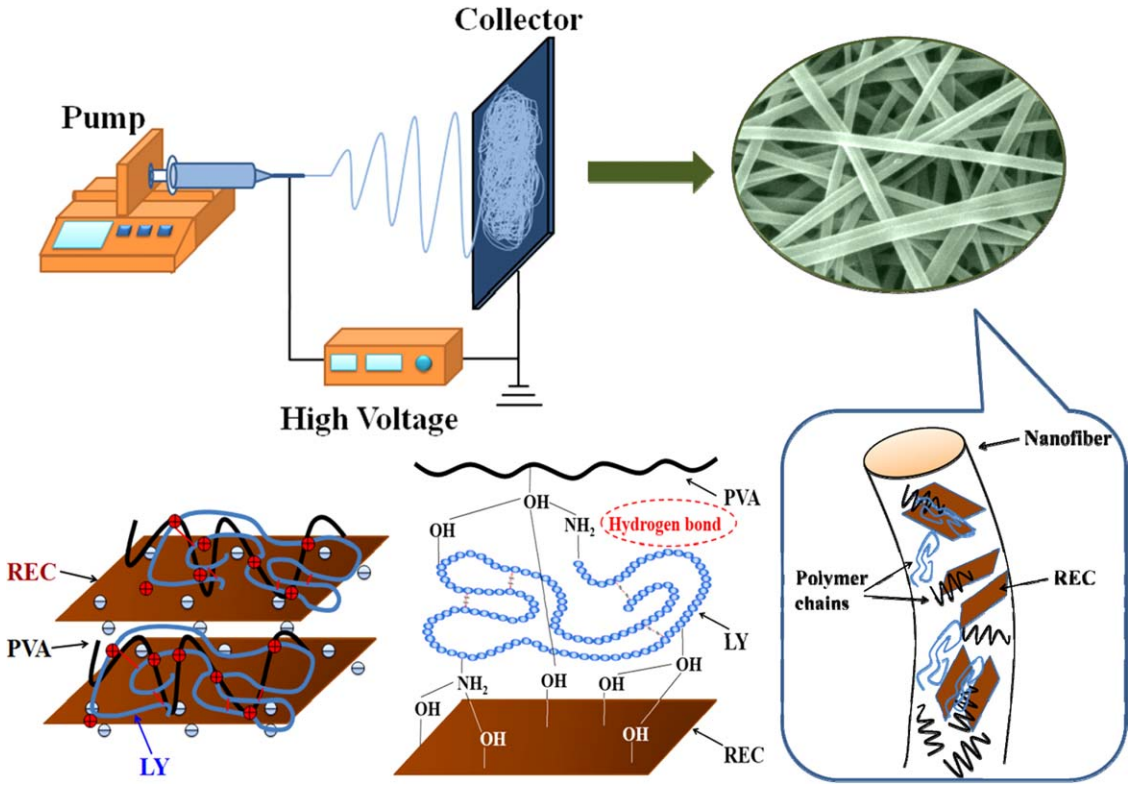

Scheme 1. Schematic diagram illustrating the fabrication of PVA/LY/REC composite nanofibrous membranes and the interaction between REC and the chains of PVA and LY. [Color figure can be viewed in the online issue, which is available at wileyonlinelibrary.com.]

biomedical applications because of its excellent chemical and physical properties, biocompatibility, low cytotoxicity, and so on.[39] But PVA itself can barely inhibit bacteria, which is certified again by Figure 8(b). The negative control samples showed weak antibacterial activity only because when these disks were covered on the surface of the bacteria colonies, the bacterial environment would lack of O_2 and CO_2, which accounted for the aptness to die off of the nearby bacteria.[3]

Apparently, the addition of LY could remarkably enhance the bacteria inhibition activity of nanofibrous membranes [Figure 8(c–e)], which might because of the remarkable antimicrobial activity of LY against both Gram-negative and Gram-positive bacteria. Besides, the degree of bacterial inhibition of nanofibrous membranes containing LY had risen with the increasing amount of LY. In addition, after adding REC, the nanofibrous membranes [Figure 8 (f,h)] exhibited stronger antibacterial activity compared with nanofibrous membranes without REC. The reasons might be as follows: first, REC, with significant adsorption capacities, could absorb and immobilize the bacteria on its surface;[7] second, the chains of LY accumulated on the surface of REC, which was similar to the interaction between CS chains and REC;[7] third, LY chains could enlarged the interlayer distance of REC, thus the contact and interaction between bacteria and antibacterial substances became more efficient.[7]

Moreover, the inhibition activity of all the membranes against the *S. aureus* were better than that against E. *coli*, regardless of what the composite nanofibrous membranes were fabricated from,[3,11] which was mainly because LY exhibited more efficient antibacterial activity against Gram-positive rather than Gram-negative bacteria as the structure of their cell walls was different. Opposite to Gram-positive bacteria, Gram-negative bacteria have thin cell wall consisting of peptidoglycan and thick outer membrane,[7] and the outer membrane composed of protein, phospholipids, and lipopolysaccharides is an adminicular barrier against the aggression of LY.[40] Additionally, Gram-negative bacteria can produce specific proteinaceous inhibitors to protect themselves from the lytic action of LY.[16] Furthermore, the difference of bacteria cell structure accounts for the difference of the adsorption action of the layered silicates against these two species of bacteria.

CONCLUSIONS

PVA/LY/REC nanofibrous membranes with enhanced antibacterial activity were prepared simply and conveniently via electrospinning. The morphologies of the as-spun nanofibrous membranes were greatly influenced by the composition of the solutions including PVA/LY weight ratios and the addition of REC. The EDX and XPS spectra verified the combination of PVA and LY as well as the existence of REC in the composite membranes. In addition, the FTIR results revealed that the hydroxyl groups of REC had intermolecular interaction with the chains of LY and PVA. Moreover, the SAXRD results and TEM images confirmed that REC in the composite membranes was exfoliated by LY. With higher surface area and the synergetic bacteria inhibition of REC, LY exfoliated REC based composite nanofibrous membranes exhibited evidently enhanced antibacterial activity. Furthermore, the addition of REC also considerably strengthened the thermal stability of the as-spun membranes.

ACKNOWLEDGMENTS

This project was funded by National Natural Science Foundation of China (Nos. 31101365 and 51473125) and partially supported by the Fund for Fostering Talents in Basic Science of the National Natural Science Foundation of China (No. J1103409) and the Open Research Fund Program of Hubei-MOST KLOS & KLOBME.

REFERENCES

1. European Food Safety Authority. *EFSA J.* **2011**, *9*, 2007.
2. Xiao, J.; Peng, T.; Dai, K.; Zan, L.; Peng, Z. *J. Solid State Chem.* **2007**, *180*, 3188.
3. Deng, H.; Lin, P.; Xin, S.; Huang, R.; Li, W.; Du, Y.; Zhou, X.; Yang, J. *Carbohydr. Polym.* **2012**, *89*, 307.
4. Shi, W.; Cheng, Q.; Zhang, P.; Ding, Y.; Dong, H.; Duan, L.; Li, X.; Xu, A. *Catal. Commun.* **2014**, *56*, 32.
5. Wu, S.; Fang, J.; Hong, X.; Hui, K. S.; Chen, Y. *Dalton Trans.* **2014**, *43*, 2611.
6. Lu, Y.; Chang, P. R.; Zheng, P.; Ma, X. *Chem. Eng. J.* **2014**, *255*, 49.
7. Wang, X.; Du, Y.; Yang, J.; Wang, X.; Shi, X.; Hu, Y. *Polymer* **2006**, *47*, 6738.
8. Wang, X.; Du, Y.; Luo, J.; Yang, J.; Wang, W.; Kennedy, J. F. *Carbohydr. Polym.* **2009**, *77*, 449.
9. Wang, X.; Du, Y.; Luo, J.; Lin, B.; Kennedy, J. F. *Carbohydr. Polym.* **2007**, *69*, 41.
10. Wang, W.; Wang, A. *Carbohydr. Polym.* **2009**, *77*, 891.
11. Deng, H.; Wang, X.; Liu, P.; Ding, B.; Du, Y.; Li, G.; Hu, X.; Yang, J. *Carbohydr. Polym.* **2011**, *83*, 239.
12. Deng, H.; Li, X.; Ding, B.; Du, Y.; Li, G.; Yang, J.; Hu, X. *Carbohydr. Polym.* **2011**, *83*, 973.
13. Parisien, A.; Allain, B.; Zhang, J.; Mandeville, R.; Lan, C. Q. *J. Appl. Microbiol.* **2008**, *104*, 1.
14. Abdou, A. M.; Higashiguchi, S.; Aboueleinin, A. M.; Kim, M.; Ibrahim, H. R. *Food Control* **2007**, *18*, 173.
15. Yu, K. H.; Kim, K. N.; Lee, J. H.; Lee, H. S.; Kim, S. H.; Cho, K. Y.; Nam, M. H.; Lee, I. H. *Dev. Compar. Immunol.* **2002**, *26*, 707.
16. Leysen, S.; Vanderkelen, L.; Weeks, S. D.; Michiels, C. W.; Strelkov, S. V. *Cell. Mol. Life Sci.* **2013**, *70*, 1113.
17. Kawai, A.; Urabe, Y.; Itoh, T.; Mizukami, F. *Mater. Chem. Phy.* **2010**, *122*, 269.
18. Kao, K. C.; Lin, T. S.; Mou, C. Y. *J. Phys. Chem. C* **2014**, *118*, 6734.
19. Uygun, M.; Uygun, D. A.; Altunbas, C.; Akgo, S.; Denizli, A. *Sep. Sci. Technol.* **2014**, *49*, 1270.
20. Huang, W.; Xu, H.; Xue, Y.; Huang, R.; Deng, H.; Pan, S. *Food Res. Int.* **2012**, *48*, 784.
21. Zhou, B.; Li, Y.; Deng, H.; Hu, Y.; Li, B. *Colloids Surf. Bioint.* **2014**, *116*, 432.
22. Yuan, S.; Yin, J.; Jiang, W.; Liang, B.; Pehkonen, S. O.; Choong, C. *Colloids Surf. Bioint.* **2013**, *106*, 11.

23. Hiwale, P.; Lampis, S.; Conti, G.; Caddeo, C.; Murgia, S.; Fadda, A. M.; Monduzzi, M. *Biomacromolecules* **2011**, *12*, 3186.
24. Zhou, Y.; Yang, H.; Liu, X.; Mao, J.; Gu, S.; Xu, W. *Int. J. Biol. Macromol.* **2013**, *53*, 88.
25. Xiao, S.; Shen, M.; Guo, R.; Huang, Q.; Wang, S.; Shi, X. *J. Mater. Chem.* **2010**, *20*, 5700.
26. Keun Son, W.; Ho Youk, J.; Lee, T. S.; Park, W. H. *Mater. Lett.* **2005**, *59*, 1571.
27. Li, W.; Li, X.; Chen, Y.; Li, X.; Deng, H.; Wang, T.; Huang, R.; Fan, G. *Carbohydr. Polym.* **2013**, *92*, 2232.
28. Li, L.; Hsieh, Y. L. *Carbohydr. Res.* **2006**, *341*, 374.
29. Vinu, A.; Miyahara, M.; Ariga, K. *J Phys Chem B* **2005**, *109*, 6436.
30. Wang, Y.; Zhang, H.; Wu, Y.; Yang, J.; Zhang, L. *Eur. Polym. J.* **2005**, *41*, 2776.
31. Fornes, T.; Hunter, D.; Paul, D. *Macromolecules* **2004**, *37*, 1793.
32. Yu, S.; Chen, C.; Chang, P.; Wang, T.; Lu, S.; Wang, X. *Appl. Clay Sci.* **2008**, *38*, 219.
33. Huang, Y.; Ma, X.; Liang, G.; Yan, Y.; Wang, S. *Chem. Eng. J* **2008**, *138*, 187.
34. Liu, X.; Wang, X.; Zhang, J.; Wang, X.; Lu, Y.; Tu, H.; Deng, H.; Jiang, L. *RSC Adv.* **2014**, *4*, 8867.
35. Liu, B.; Wang, X.; Li, X.; Zeng, X.; Sun, R.; Kennedy, J. F. *Carbohydr. Polym.* **2012**, *90*, 1826.
36. Liu, B.; Wang, X.; Pang, C.; Luo, J.; Luo,Y.; Sun, R. *Carbohydr. Polym.* **2013**, *92*, 1078.
37. Huang, R.; Li, Y.; Zhou, X.; Zhang, Q.; Jin, H.; Zhao, J.; Pan, S.; Deng, H. *Carbohydr. Polym.* **2012**, *90*, 957.
38. Zhao, L.; Mitomo, H.; Zhai, M.; Yoshii, F.; Nagasawa, N.; Kume, T. *Carbohydr. Polym.* **2003**, *53*, 439.
39. Bryaskova, R.; Pencheva, D.; Kale, G. M.; Lad, U.; Kantardjiev, T. *J Colloid Interf. Sci.* **2010**, *349*, 77.
40. Ibrahim, H. R.; Kato, A.; Kobayashi, K. *J Agri Food Chem.* **1991**, *39*, 2077.